Research Square

Preprints are preliminary reports that have not undergone peer review.
They should not be considered conclusive, used to inform clinical practice,
or referenced by the media as validated information.

An Antimicrobial Cyclic Peptide with Multitarget Efficacy for Acne

Nannan Yu
Jiangnan University
Gantong GUO
DFSIN (Shanghai) Biotechnology
Luyao Zhang
Jiangnan University
Tao He
DFSIN (Shanghai) Biotechnology
Meng Zhang
Jiangnan University
Jingting Wang
Jiangnan University
Jinfang Wang
Dermatide Biotec Pte Ltd.
Jun Yao
Dermatide Biotec Pte Ltd.
Guangli Wang
glwang@jiangnan.edu.cn
Jiangnan University
Jing Wang
Jiangnan University

Article

Keywords: Acne vulgaris, Antimicrobial cyclic peptide, Anti-acne efficacy, Transdermal permeation, Synergistic mechanism

Posted Date: June 18th, 2026

DOI: https://doi.org/10.21203/rs.3.rs-9733105/v1

License: This work is licensed under a Creative Commons Attribution 4.0 International License.
Read Full License

Additional Declarations: No competing interests reported.

Version of Record: A version of this preprint was published at Scientific Reports on October 11th, 2026.
See the published version at https://doi.org/10.1038/s41598-026-75285-7.

An Antimicrobial Cyclic Peptide with Multitarget Efficacy for Acne

Nannan Yu,[1] Gantong Guo,[2] Luyao Zhang,[1] Tao He,[2] Meng Zhang,[1] Jingting Wang,[1] Jinfang Wang,[3] Jun Yao,[3] Guang-Li Wang,[1,*] Jing Wang,[1,*]

1. Key Laboratory of Synthetic and Biological Colloids, Ministry of Education, School of Chemical & Material Engineering, Jiangnan University, Wuxi, Jiangsu, 214122, China

2. DFSIN (Shanghai) Biotechnology Co., Ltd., China

3. Dermatide Biotec Pte Ltd., 059413, Singapore

*Email: glwang@jiangnan.edu.cn;jingwang@jiangnan.edu.cn

Abstract

Acne vulgaris is a complex inflammatory disorder, and current treatment options are often limited by antibiotic resistance and cutaneous irritation, underscoring the urgent need for safer multi-target therapeutic alternatives. In this study, a novel antimicrobial cyclic peptide (AMCP) was systematically evaluated for its multidimensional anti-acne efficacy, and a penetration enhancer was developed for improving the transdermal penetration. At a concentration of 20 μg/mL, AMCP inhibited dihydrotestosterone (DHT)- and linoleic acid (LA)-induced lipid synthesis in SZ95 sebocytes by 40.0% and 29.1%, respectively. Furthermore, it exhibited potent bactericidal activity against *C. acnes* (MIC or MBC at 0.5 μg/mL) and *S. aureus* (MIC or MBC at 1.0 μg/mL). AMCP suppressed key inflammatory mediators (IL-6, IL-8, IL-1β, TNF-α, and PGE_2) in a concentration-dependent manner in both HaCaT keratinocytes and SZ95 sebocytes. Additionally, it promoted keratinocyte migration, upregulated the expression of barrier-related genes (FLG, IVL, Claudin-1, and KRT1), and downregulated KLK7 expression. Notably, the combination of 2% propylene glycol and 0.1% sodium surfactin synergistically enhanced transdermal permeation, resulting in a 5-fold increase in cumulative permeation at 8 h. In conclusion, AMCP exerts anti-acne effects through a tetra-dimensional synergistic mechanism of sebum control, antibacterial activity, anti-inflammation, and barrier repair, while also overcoming the bottleneck of transdermal delivery. These findings provide a new cyclic peptide with anti-acne efficacy, positioning AMCP as a promisingly anti-acne ingredient.

Keywords: Acne vulgaris; Antimicrobial cyclic peptide; Anti-acne efficacy; Transdermal permeation; Synergistic mechanism

1 Introduction

Acne vulgaris is a highly prevalent chronic inflammatory skin disease worldwide, primarily affecting the pilosebaceous units.[1] The pathogenesis of acne is complex, involving four core interrelated pathways: hyperseborrhoea combined to a modification of sebum composition, colonization by *Cutibacterium acnes* (*C. ances*) and *Staphylococcus aureus* (*S. aureus*), hyperkeratinization, and secreted inflammation.[2] Although commonly associated with adolescence, its incidence in the adult population has been progressively increasing in recent years.[3] Therefore, anti-acne strategies and ingredients are highly demanding.

Current clinical management of acne primarily involves topical retinoids[4], antibiotics[5], and hormonal[6]. While these treatments demonstrate efficacy to varying degrees, they possess considerable limitations. For example, long-term antibiotic use frequently elevates the risk of bacterial resistance, whereas retinoids often provoke cutaneous adverse effects—such as dryness, erythema, and desquamation—that ultimately compromise patient adherence.[7,8] Additionally, the clinical utility of physical modalities such as photodynamic therapy and laser treatment is limited by their high costs and restricted accessibility, despite their proven efficacy.[9,10] Consequently, developing new ingredients with multimodal mechanisms of action, improved biocompatibility, and a low potential for inducing resistance has become a research priority.

Antimicrobial peptides (AMPs), particularly linear AMPs, have garnered significant attention for their broad-spectrum antimicrobial activity and low propensity for inducing resistance.[11] However, their practical application in cosmetic formulations has been hampered by several limitations, including susceptibility to proteolytic degradation, low bioavailability, and potential skin irritation.[12] In contrast, the cyclization of linear peptides imparts considerable structural rigidity.[13] This modification not only enhances stable target binding but also confers resistance to proteolytic hydrolysis due to the absence of free N- and C-termini.[14] Recent studies have demonstrated the dermatological potential of antimicrobial cyclic peptides (AMCPs). For instance, daptomycin exhibits potent and rapid bactericidal activity against both drug-resistant and susceptible Gram-positive bacteria.[15] Despite

these advances, commercially available cosmetic products remain predominantly based on linear peptides, with limited documentation on the development and application of cyclic variants. In contrast, cyclic peptides—offering superior structural stability, biocompatibility, and transdermal permeability—hold substantial promise for future cosmetic applications.

This study focused on a promising AMCP, comprising 28 amino acid residues with the sequences of CEWYNISCQLGNKGQWCTLTKECQRSCK, an average molecular weight of 3310.80 Da, and a molecular formula of $C_{139}H_{217}N_{41}O_{43}S_5$, for which the multidimensional efficacy and transdermal behavior were systematically investigated. The research methodology included: (i) evaluating its sebum-controlling, anti-inflammatory, and barrier-repairing functions using HaCaT and SZ95 models; (ii) determining its minimum inhibitory concentration (MIC) and minimum bactericidal concentration (MBC) via the microbroth dilution method; (iii) assessing its transdermal permeation characteristics using Franz diffusion cell experiments with various penetration enhancers. This study represents the first systematic integration of an AMCP into acne skincare, marking a departure from the then-prevailing technological landscape dominated by linear peptides. By leveraging its superior stability, biocompatibility, and multi-target binding capacity, this cyclic peptide scaffold enables a quad-effect anti-acne mechanism that simultaneously targets sebum overproduction, microbial colonization, inflammatory cascades, and epidermal barrier dysfunction. Furthermore, when combined with a tailored permeation-enhancement strategy, the AMCP demonstrates markedly improved transdermal permeability. Collectively, these findings provide an experimental foundation for the development of cyclic peptide-based new ingredients for anti-acne cosmetic applications.

2 Materials and Methods

2.1 Chemicals and Reagents

The specified AMCP was obtained from Sinagri Yingtai Bio-Peptide Co., Ltd. (Henan, China). The immortalized human keratinocyte cell line (HaCaT) was obtained from Cell Bank of Type Culture Collection of Chinese Academy of Sciences China (Shanghai, China). The human sebaceous gland

cells were provided by Professor Christos C. Zouboulis (Faculty of Medicine, Freie Universität Berlin, Germany). *C. acnes* (ATCC 6919) and *S. aureus* (ATCC 6538) were obtained from Shanghai Center of Bioresource Collection (Shanghai, China). Freshly thawed miniature pig skin was purchased from Aperture Biotechnology Co., Ltd. (Shandong, China). High-glucose dulbecco's modified eagle medium (DMEM), fetal bovine serum (FBS), and 0.25% trypsin were acquired from Gibco^{TM} (Thermo Fisher Scientific, Inc., Waltham, MA, USA). Phosphate-buffered saline (PBS) and penicillin-streptomycin solution were obtained from HyClone Laboratories, Inc. (Logan, UT, USA). 3-(4,5-Dimethylthiazol-2-yl)-2,5-diphenyltetrazolium bromide (MTT) was purchased from Sigma-Aldrich (St. Louis, MO, USA). Dihydrotestosterone (DHT) was obtained from Haoyang Biotechnology Co., Ltd. (Shanghai, China). Linoleic acid (LA), dimethyl sulfoxide (DMSO) and N, N'-dimethylformamide (DMF) were acquired from National Pharmaceutical Group Corporation (Sinopharm) Chemical Reagent Co., Ltd. (Beijing, China). Nile red was purchased from InnoChem Science & Technology Co., Ltd. (Beijing, China). Cation-Adjusted Mueller-Hinton Broth (CAMHB) and Mueller-Hinton Broth (MHB) were obtained from Baishengyue Biotechnology Co., Ltd. (Shanghai, China). ELISA kits for detecting interleukin-6 (IL-6), interleukin-8 (IL-8), interleukin-1 β (IL-1β) prostaglandin E_2 (PGE_2) and tumor necrosis factor-alpha (TNF-α), were purchased from Shanghai Universal Biotech Co., Ltd. (Shanghai, China). Total RNA extraction reagent (TRIzol) was purchased from Thermo Fisher Scientific (Waltham, MA, USA). Fluorescein isothiocyanate (FITC) was purchased from Shanghai Aladdin Biochemical Technology Co., Ltd. (Shanghai, China). Optimum Cutting Temperature Compound (OTC) was obtained from Beyotime Biotechnology Co., Ltd. (Shanghai, China).

2.2 Cell Cultures

HaCaT and SZ95 cells were both cultured at 37℃ in a humidified CO_2 incubator (95% air, 5% CO_2, Bosun Medical Biological Instrument Co., Ltd. Shanghai, China) in DMEM supplemented with 10% FBS.

2.3 Sebum Control Effects of AMCP

2.3.1 Assessment of Viability

The SZ95 cells (1.5×10^5/mL) were collected and seeded into 96-well plates with 100 μL per well. After being cultured for 24 h, the experimental groups were treated with 100 μL of AMCP solutions at different concentrations (10, 20, 50, 60, 80, 100 μg/mL), respectively. The stimulation groups were treated with 100 μL of DHT solutions at different concentrations (5, 10, 25, 50, 100 μg/mL) or different concentrations (2, 10, 15, 50, 100, and 150 μg/mL) of LA solution, respectively. The control group was treated with 100 μL of DMEM. After incubating them for 24 h and discarding the culture medium, 100 μL of 0.5 mg/mL MTT solution was added to each well. After 4 h, 100 μL of DMSO solution was added to each well to dissolve the formazan crystals. Finally, the absorbance of each well was measured at an absorbance of 490 nm. Cell viability was calculated using the following formula:

$$\text{Cell viability (\%)} = (OD_T/OD_B) \times 100\%$$

Where: OD_T and OD_B represented the average OD values of the experimental and the blank groups at 490 nm, respectively.

2.3.2 Lipid Content Assay

Nile red staining was employed to quantitatively detect lipids in SZ95 sebocytes. DMEM served as the control group, while LA or DHT was used as the stimulant model group. The experimental group consisted of co-treatment with different mass concentrations of AMCP solution along with 10 μg/mL of DHT or 75 μg/mL of LA. After incubation for 48 h, Nile red solution (10 μg/mL) was added, followed by incubation at 37 ℃ in the darkness for 20 min. Lipid droplets in cells were visualized using Olympus IX73 Inverted Research Microscope (Olympus Corporation., Tokyo, Japan) and corresponding fluorescence intensities for quantitative analysis were measured using multimode microplate reader (Allsheng Instruments Co., Ltd. Hangzhou, China) under the excitation/emission wavelengths of 485 and 565 nm.

$$\text{Lipid synthesis ratio (\%)} = (FI_T/FI_B) \times 100\%$$

Where: FI_T and FI_B were the average fluorescence intensities of the experimental and control groups, respectively.

2.4 Antibacterial Activities *In Vitro*

Antibacterial effects of AMCP were tested against bacterial strains including *C. acnes* and *S. aureus* by measuring MIC and MBC values. The following controls were established in a sterile 96-well plate: CAMHB alone served as the negative control, while medium containing bacterial suspension served as the positive control. For the test wells, 50 μL of serially diluted AMCP solutions (0.125, 0.25, 0.5, 1.0, 2.0, 4.0, 8.0, 16, 32, and 64 μg/mL) were added, followed by 50 μL of bacterial suspension to achieve a final bacterial concentration of approximately 5×10^5 CFU/mL. The 96-well plates were incubated at 37°C under appropriate conditions: *C. acnes* was cultured anaerobically for 2–3 days, while *S. aureus* was cultured aerobically for 20 h. The MIC values were determined as the lowest concentration that visually inhibited growth of the tested bacteria. After determination of the MIC values, the MBC values were determined as follows: 50 μL of all tubes not showing visible growth were subcultured on Mueller-Hinton agar (MHA) plates and incubated under the same conditions. The lowest concentration that showed at least 99.9% growth inhibition was defined as the MBC. All tests were performed in triplicate.

2.5 Anti-Inflammatory Effects of AMCP

2.5.1 Preparation of Heat-Killed *C. acnes*

C. acnes bacterial suspension was collected and washed three times with ice-cold PBS by centrifugation at 2500 rpm for 5 min each. The resulting bacterial pellet was resuspended in PBS. To prepare heat-killed bacteria, the suspension was heated in a water bath at 80°C for 30 min, followed by centrifugation at 10,000 rpm for 5 min at 4°C. The supernatant was discarded, and the bacterial pellet was collected for subsequent use.

2.5.2 Assessment of Viability

SZ95 or HaCaT cells (1.5×10^5/mL) were seeded in 96-well plates (100 μL/well). After 24 h of incubation, experimental groups received 100 μL heat-killed C. acnes at various concentrations (1×10^6,

7×10^6, 1×10^7, 7×10^7, 1×10^8, and 7×10^8 CFU/mL); while the control group received 100 μL of DMEM. Following 24 h of incubation, medium was removed and 100 μL MTT (0.5 mg/mL) was added. After 4 h, 100 μL DMSO was added to dissolve formazan crystals. Finally, the absorbance was measured at 490 nm.

2.5.3 Determination of Secretion of Inflammatory Factors (IL-6, IL-8, IL-1β, TNF-α, and PGE_2)

SZ95 or HaCaT cells (1.0×10^5 cells/mL) were collected and seeded into 24-well plates (0.5 mL/well). After 24 h of incubation, the cells were pretreated for 2 h with DMEM containing varying concentrations of AMCP (0, 10, 15, and 30 μg/mL), followed by stimulation with heat-killed *C. acnes* at a final concentration of 1×10^7 CFU/mL for 24 h. All treatments were performed in triplicate. Finally, the levels of inflammatory factors, including IL-6, IL-8, IL-1β, TNF-α, and PGE_2, were determined using ELISA kits according to the manufacturer's instructions.

2.6 Transcriptomics Analysis

The mRNA isolation and sequencing were performed by Shanghai Majorbio Bio-pharm Technology Co., Ltd. (Shanghai, China). Briefly, total RNA was extracted using the TRIzol reagent, followed by enrichment with Oligo (dT) beads and fragmentation. The fragmented RNA was then subjected to reverse transcription and second-strand cDNA synthesis. After end repair and 3'-end adenylation to facilitate efficient adapter ligation, the double-stranded cDNA was purified, size-selected, and amplified via PCR to construct the sequencing library. Sequencing was conducted on the NovaSeq X Plus platform. The raw reads underwent quality control via fastp 1.0, during which low-quality reads were eliminated to obtain clean reads. The resulting clean reads were mapped to the reference genome using HISAT2 2.0.4 to acquire mapped reads, providing the foundation for downstream analyses such as transcript assembly and expression level quantification. DESeq2 was subsequently employed to screen for differentially expressed genes (DEGs) based on read counts, applying stringent criteria of $|\log_2(\text{fold change})| > 1$ and a false discovery rate (FDR) < 0.05. Finally, to comprehensively interpret their biological implications, the identified DEGs were annotated with Gene Ontology (GO) terms and

subjected to Kyoto Encyclopedia of Genes and Genomes (KEGG) pathway enrichment analysis. GO annotation analysis and KEGG pathway analysis were carried out by Diamond and KOBAS, respectively.

2.7 Skin Barrier-Repairing Effects of AMCP

2.7.1 Cell Scratch Assay

HaCaT cells were seeded into 6-well plates and cultured until reaching approximately 90% confluence. A uniform scratch wound was then created in each monolayer using a sterile 200 μL pipette tip held perpendicular to the plate bottom. After scratching, the cells were gently washed twice with PBS to remove detached debris. The experimental groups were replenished with medium containing AMCP at specified concentrations (5.0 and 10 μg/mL), while the control group received DMEM. The plates were returned to the incubator for further culture and scratches were observed and imaged under an inverted microscope at 0, 12, and 24 h post-scratch. Scratches widths were quantitatively measured using Image J software.

2.7.2 RT-PCR analysis

Total RNA was extracted from the treated cells using an RNA extraction kit The purity and concentration of the isolated RNA samples were assessed using a Nanodrop 2000 spectrophotometer (Thermo Fisher Scientific, Erlangen, Germany). The extracted RNA was then used to generate cDNA using a PCR machine (Eastwin Life Sciences Inc., Beijing, China). The cDNA served as a template for real-time PCR amplification (Bio-Rad, Hercules, CA, USA), which was performed over 40 cycles. The thermal cycling conditions consisted of denaturation at 95 °C for 15 s, followed by annealing and extension at 60 °C for 30 s. The primers for different barrier-related proteins are listed in **Error! Reference source not found.**.

Table 1. Primers Sequence

Cell	Gene	Primers（5'-3'）
HaCaT	FLG	F: GGATGAAGCCTATGACACCACT
		R: AACTCTGGATCCCCTACGCT

	IVL	F: GTTCCTCCTCCAGTCAATACCCA
		R: CACATTCTTGCTCAGGCAGTCC
	KLK7	F: GGACTGCACGAAGGTTTACAAGG
		R: TGTAGACTCCTGGGTCATTGGGT
	KRT1	F: TGACAAGGTGAGGTTCCTGGAG
		R: TGATGAATGACTCAAAGTAGGGCT
	Claudin1	F: TGCCCCAGTGGAGGATTTACT
		R: CCACAAAGATTGCTATCACTCCC
	GAPDH	F: CACCCAGCACAATGAAGATCAAGAT
		R: CCAGTTTTTAAATCCTGAGTCAAGC

2.8 *In vitro* Transdermal Absorption

2.8.1 FITC Labeling and Quantification of the AMCP

FITC was dissolved in DMF to prepare a 10 mg/mL stock solution. Separately, AMCP powder was dissolved in PBS to obtain a 0.2% (w/v) stock solution. The two solutions were mixed at a molar ratio of 1:10 (AMCP : FITC) and incubated with shaking for 24 h to allow complete conjugation. Following the reaction, an equal volume of distilled water was added, and the mixture was centrifuged to remove excess unreacted dye. The supernatant was collected, transferred into a dialysis bag, and dialyzed to eliminate DMF, yielding an aqueous solution of the AMCP–FITC conjugate. The fluorescence intensity of the labeled conjugate was measured using a multifunctional plate reader in fluorescence intensity mode, with excitation and emission wavelengths set at 488 nm and 525 nm, respectively.

2.8.2 *In Vitro* Skin Permeation

The transdermal permeation of AMCP in vitro was determined using the Franz diffusion method. [16] Freshly thawed miniature pig skin was immersed in physiological saline for 30 min, then trimmed to an appropriate size and mounted between the donor and receptor compartments, with the stratum corneum facing the donor side and the dermis facing the receptor side. Both compartments were filled with PBS, and care was taken to eliminate air bubbles during assembly. The donor compartment was sealed with Parafilm, while the receptor compartment was equipped with a magnetic stir bar. The system was maintained at 37 ± 0.5 °C with a stirring rate of 300 rpm. Each group was tested in triplicate.

The cumulative permeated amount (Q_n) and cumulative permeation ratio (η) were calculated according to the following formulas:

$$Q_n = C_n V + \sum_{i=1}^{i=n-1} C_i V_i$$

$$\eta = Q_n / 800 \times 100\%$$

Where: Q_n: cumulative amount permeated (μg); C_n: mass concentration of the sample at the n-th sampling (μg/mL); V: volume of the receptor compartment (mL); V_i: volume of the sample withdrawn at the i-th sampling (mL); η: cumulative permeation ratio (%).

2.8.3 Skin Sectioning and Fluorescence Imaging

Following the transdermal permeation experiment, the skin samples were retrieved and sequentially rinsed with distilled water and physiological saline. The specimens were then embedded in OCT compound. Using a cryostat microtome (CM1860UV, Leica, Germany), 20 μm-thick sections were prepared. These sections were observed under Olympus IX73 Inverted Research Microscope and images were captured to visually assess the distribution of AMCP across different skin layers.

2.9 Statistical Analysis

The data were analyzed by GraphPad (GraphPad Prism 10.3.1, GraphPad Software, LLC, Boston, MA, USA), and the data were expressed as mean ± standard deviation. Comparison between groups using analysis of variance (ANOVA) after Tukey test. A p-value less than 0.05 was considered to be statistically significant.

3 **Results**

3.1 Sebum Control Effects of AMCP

An MTT assay was performed to determine the cytotoxicity of AMCP, LA, and DHT in SZ95 sebocytes. The results were presented in **Error! Reference source not found.**. The AMCP maintained a cell viability above 80% at concentrations below 20 μg/mL. Similarly, DHT and LA preserved cell viability above 70% at concentrations below 10 μg/mL and 150 μg/mL, respectively. Therefore, subsequent experiments utilized 10 μg/mL of DHT and 100 μg/mL of LA as stimulant concentrations, and $\leqslant$ 20 μg/mL for AMCP was adopted as working concentrations for further studies.

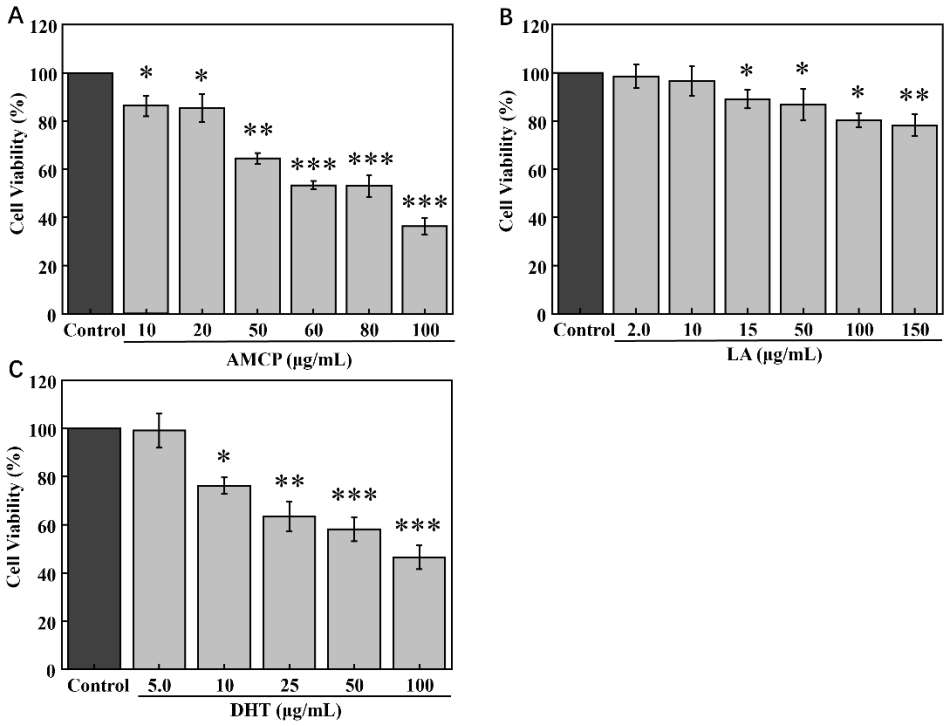

Figure 1. Effects of AMCP (A), LA (B), and DHT (C) on cell viability of SZ95 sebocytes. The error bars represent the standard deviation of three independent culture results (*, ** and *** indicate $p < 0.05$, 0.01 and 0.001 vs. control group).

Lipid dysregulation within the sebaceous gland is a key factor in the pathogenesis of acne vulgaris.[17] Therefore, this study employed Nile red staining to evaluate the inhibitory effect of the AMCP on lipid secretion on SZ95 sebocytes. As shown in **Error! Reference source not found.**, compared with the blank control group, stimulation with 10 μg/mL DHT significantly increased the fluorescence intensity, while co-treatment with AMCP resulted in a marked reduction in fluorescence intensity. In the group treated with 20 μg/mL AMCP, the inhibition ratio reached 40.0% ($p < 0.001$), indicating a significant suppressive effect. In the 100 μg/mL of LA stimulation model, the fluorescence intensity was also significantly enhanced. Similarly, co-treatment with AMCP led to a clear decrease in fluorescence intensity. In this model, the inhibition ratio observed with 20 μg/mL AMCP was 29.1% ($p < 0.01$), demonstrating a measurable inhibitory effect.

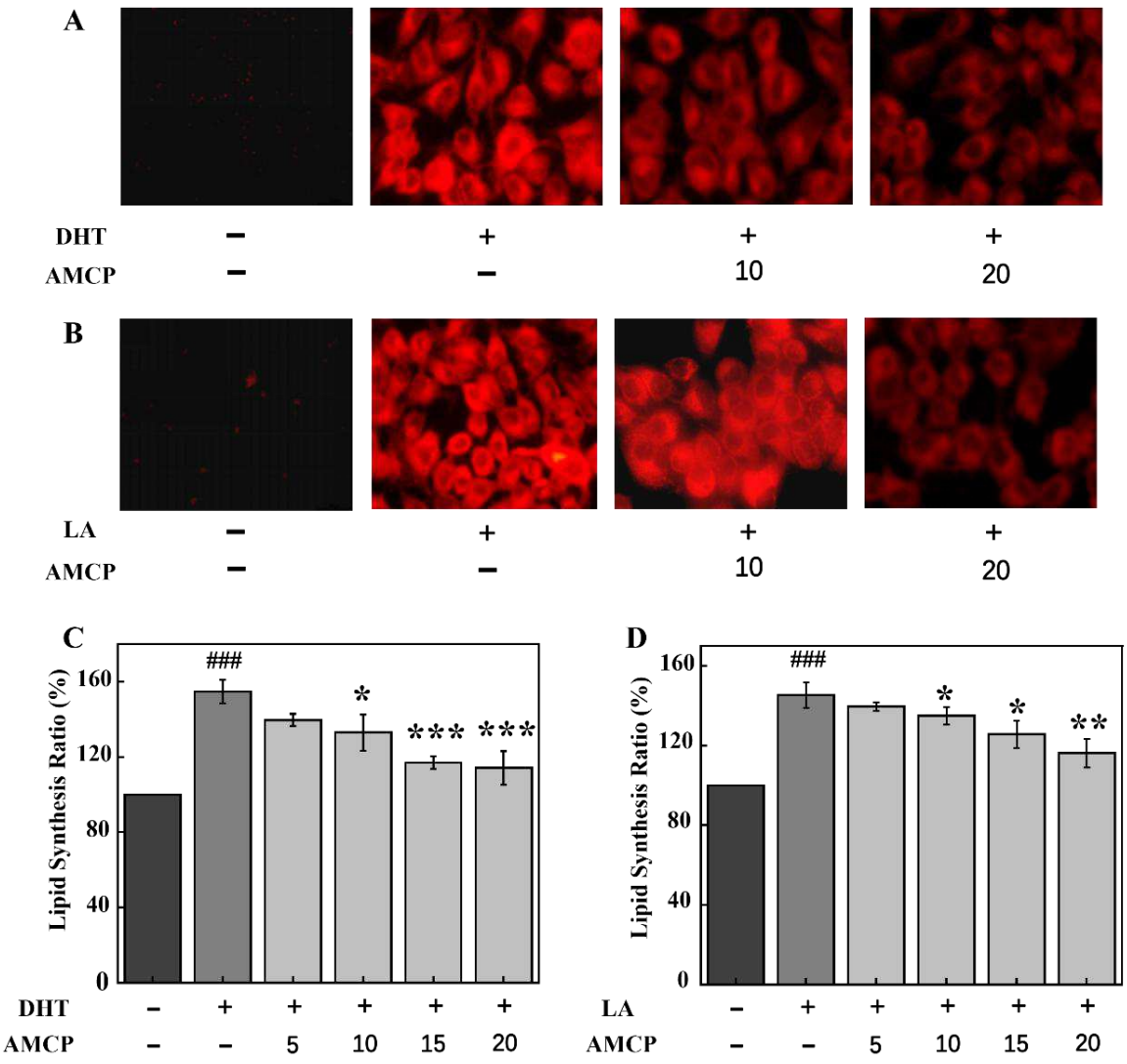

Figure 2. Nile red fluorescence staining images of SZ95 cells by LA stimulating (A) or DHT stimulating (B). Effects of AMCP on lipid synthesis in SZ95 cells by LA stimulating (C) and DHT stimulating (D). The concentration of DHT was 10 μg/mL, the concentration of LA was 100 μg/mL, and the concentration of AMCP was expressed in μg/mL. The error bars represent the standard deviation of three independent culture results (*, ** and *** indicate $p < 0.05$, 0.01 and 0.001 vs. model group; ### indicates $p < 0.001$ vs. control group).

3.2 Antibacterial Activities *In Vitro*

The over proliferation of *C. acnes* is considered one of the primary triggers of acne, as it can activate corticotropin-releasing hormone pathways, leading to excessive sebum production.[18] Consequently, inhibiting the overgrowth of *C. acnes* is a common strategy in most acne treatments. In this study, the

broth microdilution method was employed to determine the MIC and the MBC of the AMCP and the results are presented in **Error! Reference source not found.**.

Table 2 Results of determination of MIC values and MBC values.

Bacterial Strain	MIC（μg/mL）	MBC（μg/mL）
S. aureus	1.0	1.0
C. acnes	0.5	0.5

As shown in **Error! Reference source not found.**, the MIC values of the AMCP against *C. acnes* and *S. aureus* were 0.5 μg/mL and 1.0 μg/mL, respectively, while the corresponding MBC values were also 0.5 μg/mL and 1.0 μg/mL. These results indicated that the AMCP, at specific concentrations, exhibited significant antibacterial effects against both bacterial strains in vitro.

3.3 Anti-Inflammatory Effects of AMCP

Transcriptomic analysis was performed to preliminarily elucidate the anti-inflammatory potential of AMCP. As shown in **Error! Reference source not found.** A, 34 proteins were up-regulated and 129 ones were down-regulated.

GO annotation analysis was performed to systematically characterize the biological functions of the DEGs across three dimensions: Biological Process (BP), Cellular Component (CC), and Molecular Function (MF). As illustrated in **Error! Reference source not found.**B, within the BP category, the DEGs were significantly enriched in processes related to cellular processes and biological regulation. In the CC category, they were predominantly associated with fundamental cellular structures and protein-functional complexes. Regarding MF, the DEGs were primarily involved in binding and catalytic activity. Collectively, these findings suggest that the DEGs may play broad roles in regulating essential cellular physiological activities.

Further KEGG pathway enrichment analysis (**Error! Reference source not found.** C) revealed that the DEGs were significantly enriched in 20 signal transduction pathways ($p < 0.05$), including the IL-17 signaling pathway, MAPK signaling pathway, NF-κB signaling pathway, and Toll-like receptor signaling pathway Notably, several of these—namely the IL-17, MAPK, NF-κB, and Toll-like receptor

signaling pathways—are well-established as key regulators of inflammatory responses.[19 -21] These findings further support the potential role of the antimicrobial peptide in modulating inflammation through the MAPK and NF-κB pathways.

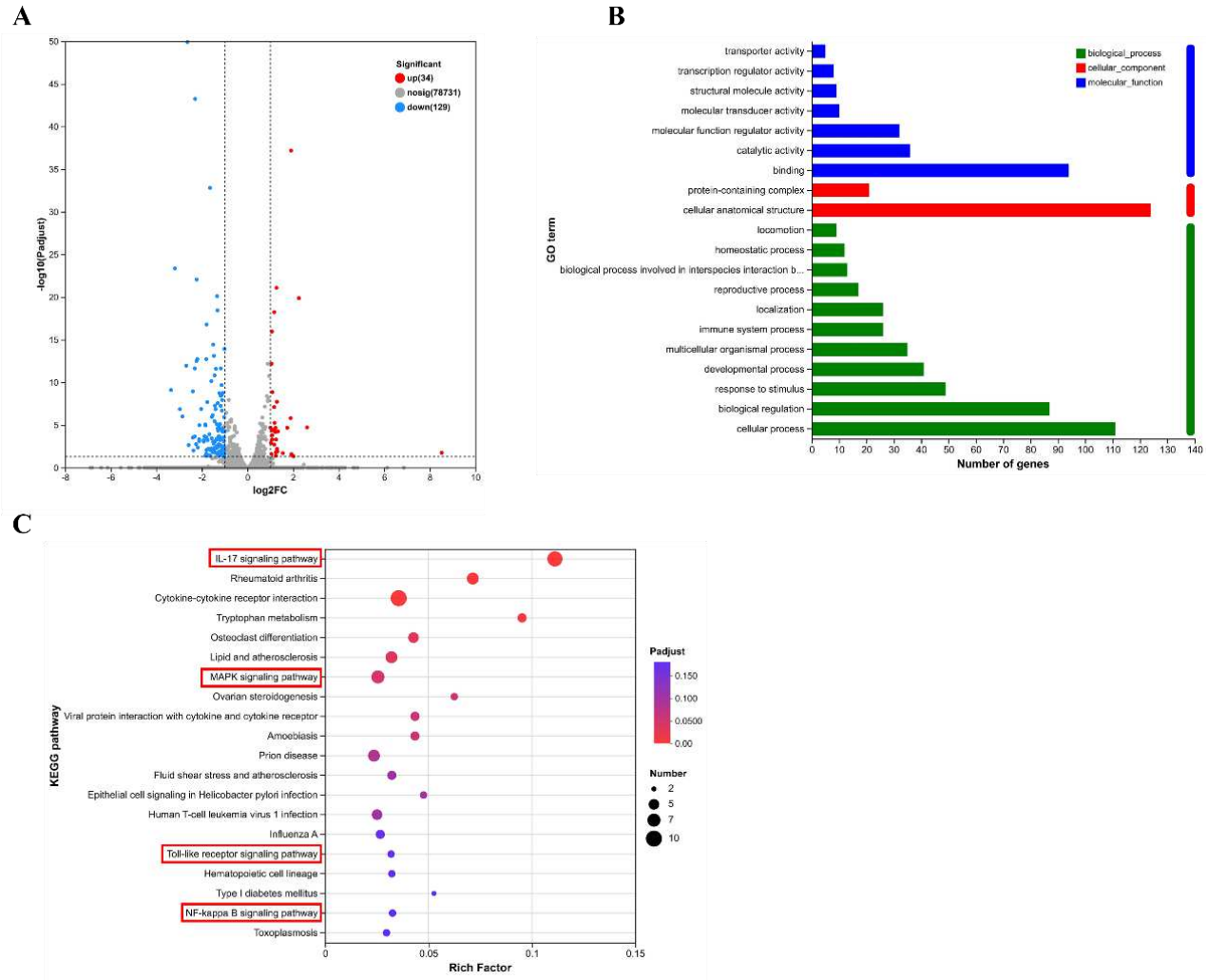

Figure 3. Transcriptomic analysis of HaCaT Cells stimulated by heat-killed *C. acnes*: (A) Volcano plot of DEGs; (B) GO annotation analysis of DEGs; (C)KEGG enrichment analysis of DEGs.

To investigate the anti-inflammatory effects of AMCP, we established an in vitro inflammation model by stimulating HaCaT and SZ95 cells with heat-killed *C. acnes*. In this model, the impact of AMCP on the expression of key pro-inflammatory mediators (IL-6, IL-8, IL-1β, TNF-α, and PGE_2) was subsequently examined.

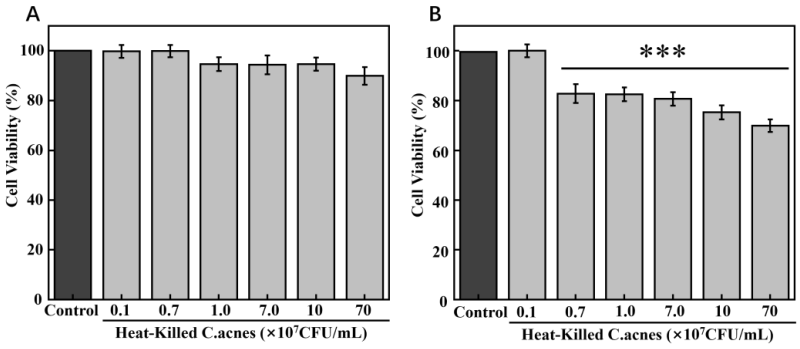

Figure 4. Effects of different concentrations of heat-killed *C. acnes* on the viability of SZ95 cells (A) and HaCaT cells (B). The error line represents the standard deviation of three independent culture results (*, ** and *** indicate $p < 0.05$, 0.01 and 0.001 vs. control group).

Based on the MTT assay results (**Error! Reference source not found.**), heat-killed *C.acnes* did not exhibit significant cytotoxicity toward HaCaT and SZ95 cells at concentrations below 7×10^7 CFU/mL. Therefore, a concentration of 1×10^7 CFU/mL was selected for establishing the inflammatory model in subsequent experiments.

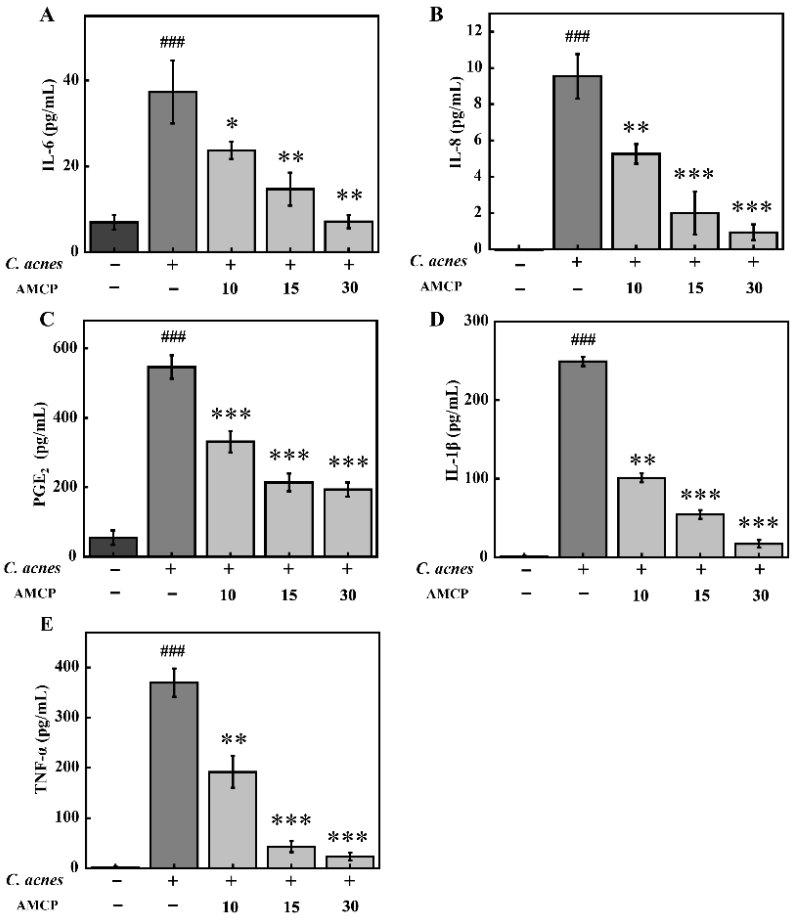

Figure 5. Effects of AMCP on the levels of IL-6 (A), IL-8 (B), PGE_2 (C), TNF-α (D), and IL-1β (E) on HaCaT keratinocytes stimulated by heat-killed *C. acnes*. The concentration of AMCP was expressed in μg/mL. The error bars represent the standard deviation of three independent culture results (*, ** and *** indicate $p < 0.05$, 0.01 and 0.001 vs. model group, ### indicates $p < 0.001$ vs. control group).

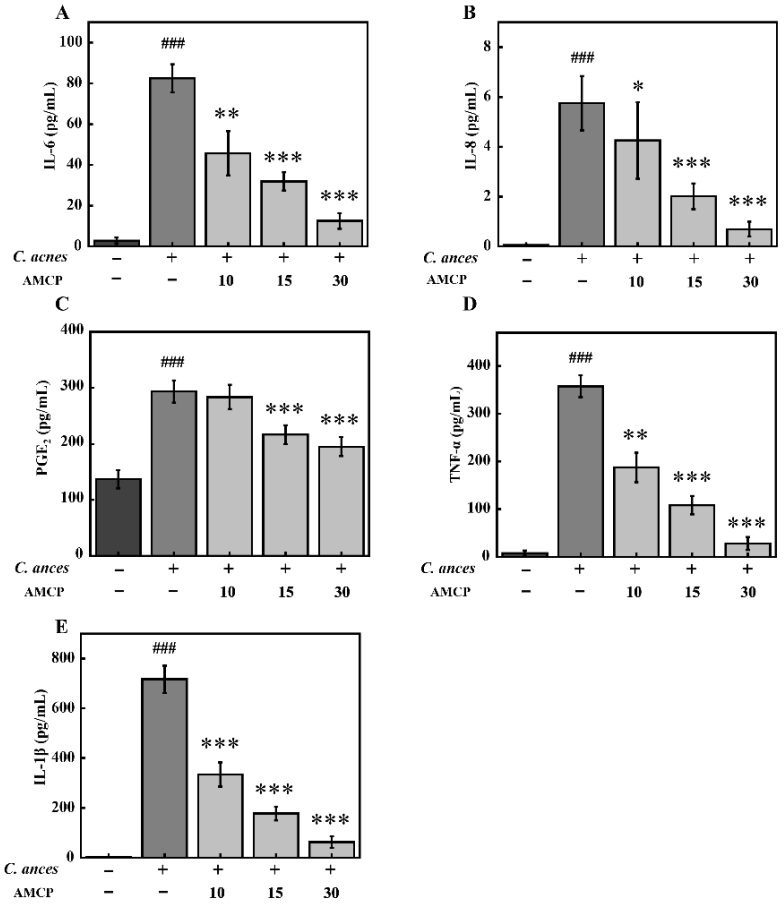

Figure 6. Effects of AMCP on the levels of IL-6 (A), IL-8 (B), PGE_2 (C), TNF-α (D), and IL-1β (E) in SZ95 sebocytes stimulated by heat-killed *C. acnes*. The concentration of AMCP was expressed in μg/mL. The error bars represent the standard deviation of three independent culture results (*, ** and *** indicate $p < 0.05$, 0.01 and 0.001 vs. model group, ### indicates $p < 0.001$ vs. control group).

Measurement of key pro-inflammatory cytokines revealed that heat-killed *C. acnes* at 1×10^7 CFU/mL significantly promoted the secretion of IL-6, IL-8, IL-1β, TNF-α, and PGE_2 in both HaCaT (**Error! Reference source not found.**) and SZ95 cells (**Error! Reference source not found.**)

compared to the blank control group. In contrast, treatment with AMCP suppressed the release of these pro-inflammatory cytokines in a concentration-dependent manner. At 30 μg/mL, AMCP markedly reduced the levels of all measured mediators in both cell types. Specifically, in HaCaT keratinocytes, the levels of IL-6, IL-8, PGE_2, IL-1β, and TNF-α were decreased by 81.0%, 90.1%, 64.6%, 93.1%, and 96.4%, respectively. In SZ95 sebocytes, corresponding reductions of 84.8%, 89.1%, 33.4%, 91.2%, and 92.1% were observed. Collectively, these findings demonstrated that AMCP exerted potent anti-inflammatory effects and effectively attenuated the inflammatory response induced by *C. acnes*.

3.4 Skin Barrier-Repairing Effects of AMCP

Acne severely disrupts skin barrier integrity through the induction of abnormal follicular keratinization, the exacerbation of inflammatory responses, and the degradation of intercellular lipids.[22] Based on this, this study evaluated the repair effect of the AMCP on the damaged skin barrier using a cell scratch assay. Results of the cell scratch assay were shown in **Error! Reference source not found.**. Treatment with 10.0 μg/mL AMCP significantly promoted HaCaT cell migration, with scratch closure rates of 35.73% ($p < 0.05$) and 60.01% ($p < 0.01$) at 12 h and 24 h, respectively, both significantly higher than the blank control group. These results demonstrate that AMCP enhances keratinocyte migration, supporting its potential role in skin barrier repair.

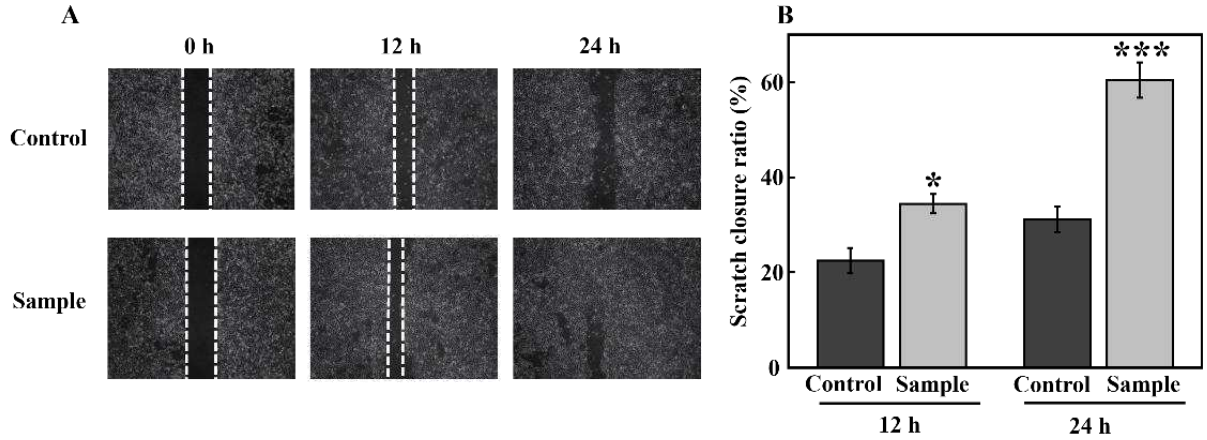

Figure 7. Effects of different concentrations of AMCP on the migration ability of HaCaT cells. The error bars represent the standard deviation of three independent culture results (* and *** indicate $p < 0.05$ and 0.001 vs. control

group).

To evaluate the skin barrier repair potential of AMCP, the key proteins (FLG, IVL, Claudin-1, KRT1, and KLK7) in barrier function were tested by their relative expressions. As shown by RT-PCR results in Figure 8, AMCP treatment significantly increased the relative expression of FLG, IVL, Claudin-1, and KRT1 compared to the model group, while markedly suppressing KLK7 relative expression. Specifically, after treatment with 15 μL/mL AMCP, the levels of FLG, IVL, Claudin-1, KRT1 and KLK7 were increased by 104%, 37%, 30%, 208%, and 43%, respectively, accompanied by a 27% reduction in KLK7 expression.

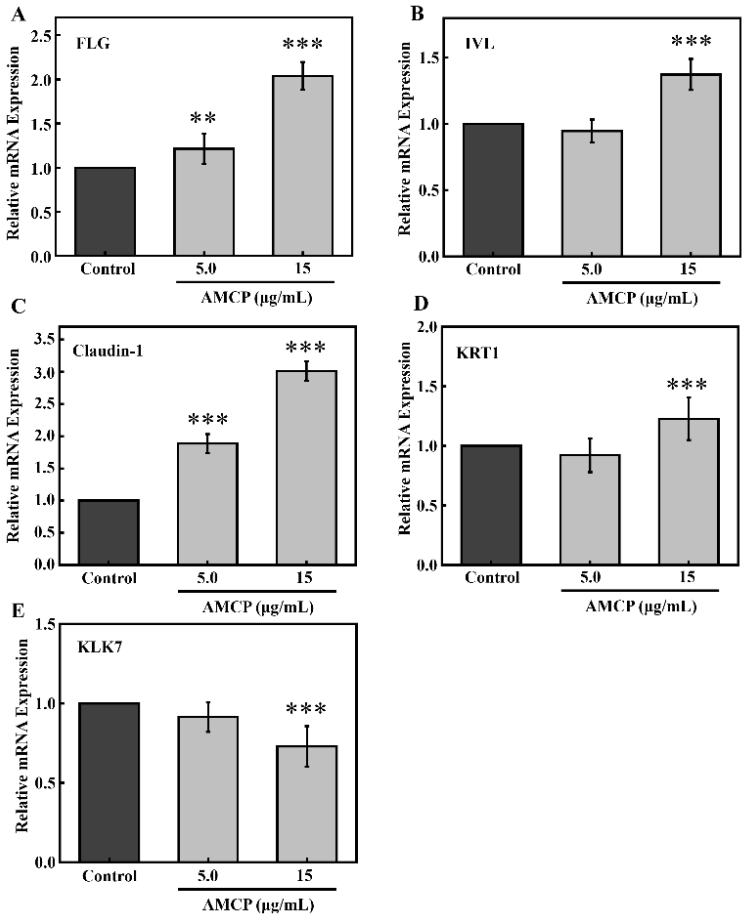

Figure 8. Effects of AMCP on the mRNA level of FLG (A), IVL (B), Claudin-1 (C), KRT1 (D) and KLK7 (E). The error bars represent the standard deviation of three independent culture results (*, ** and *** indicate $p < 0.05$, 0.01 and 0.001 vs. model group, ### indicates $p < 0.001$ vs. control group).

3.5 Transdermal Permeation of AMCP

The transdermal permeation behavior of AMCP (0.08% (w/v)) was systematically evaluated using Franz diffusion cells and an ex vivo porcine skin model under various penetration enhancer conditions. The standard curve and cumulative permeation profile of AMCP are presented in **Error! Reference source not found.**. Compared to the enhancer-free control group, all formulations containing penetration enhancers exhibited higher cumulative permeation rates, which increased progressively over time. Among these, the mixture of 2.0% propylene glycol and 0.1% sodium surfactin demonstrated the most pronounced enhancing effect, maintaining the highest cumulative permeation throughout the experiment. At 8 h, the permeation efficiency of this mixture group was five-fold higher than that of the control, indicating a synergistic interaction between propylene glycol and sodium surfactin in promoting the transdermal delivery of the cyclic peptide. From a formulation perspective, these findings highlight the potential of a composite penetration-enhancement strategy to improve the bioavailability of cyclic peptides, providing an experimental foundation for their efficient delivery in topical anti-acne applications.

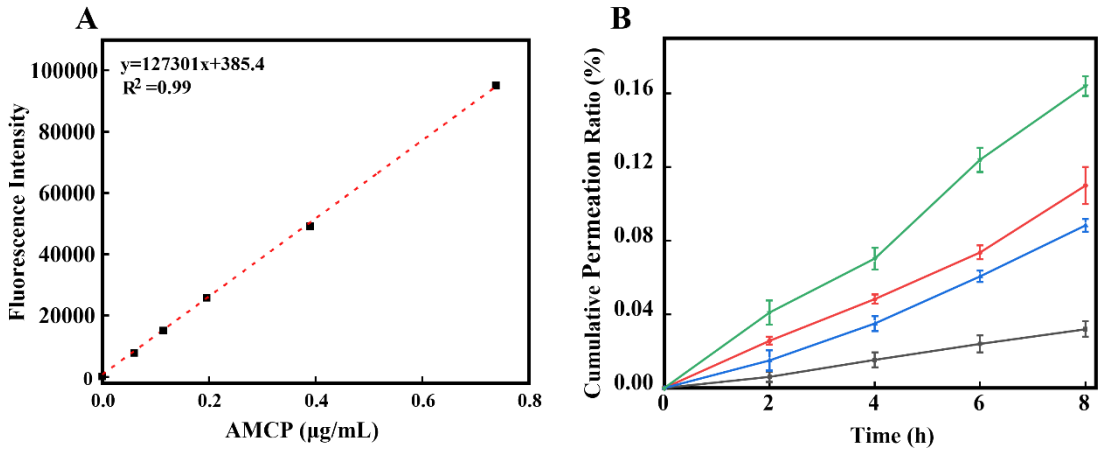

Figure 9. (A) Standard curve of the AMCP quantification; (B) Cumulative permeation profile of 0.08% (w/v) antimicrobial peptide under different penetration enhancer conditions (The groups are, from bottom to top: without penetration enhancer group, 2% propylene glycol group, 0.1% surfactin sodium group, and 0.1% surfactin sodium + 2% propylene glycol group.). The error bars represent the standard deviation of three independent culture results.

To further corroborate the transdermal permeation behavior observed in the Franz diffusion cell experiments, the distribution of AMCP within the epidermis is presented in **Error! Reference source not found.**. The FITC-labeled AMCP exhibited green fluorescence under blue light excitation. In the control group without penetration enhancer treatment, fluorescence was predominantly localized to the stratum corneum, indicating that most of the AMCP was retained within this dense barrier layer and failed to permeate effectively into the deeper epidermis. In contrast, treatment with 2.0% propylene glycol, 0.1% sodium surfactin, or their combination all resulted in significant distribution within the stratum corneum compared with the control group; notably, the combination group showed more pronounced localization in the deep epidermis. Collectively, these findings corroborate the transdermal permeation results and underscore the marked advantage of sodium surfactin in enhancing the percutaneous penetration of AMCP.

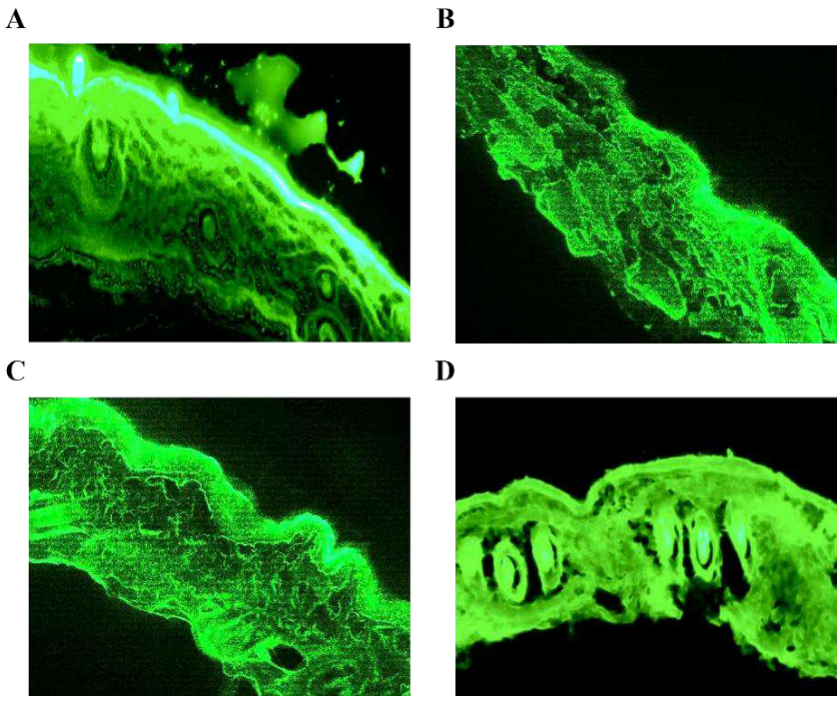

Figure 10. Distribution of the AMCP in the epidermis. (A) Control group; (B) 2.0% propylene glycol group; (C) 0.1% surfactin sodium group; (D) 0.1% surfactin sodium + 2.0% propylene glycol group.

4 Discussion

This study demonstrates that the AMCP exhibits a multi-target profile against acne pathogenesis. The AMCP shows synergistic effects across four key pathogenic dimensions of acne: sebum-

controlling, antibacterial, anti-inflammatory, and skin barrier-repairing activities, with its skin penetration enhanced through formulation optimization. A schematic diagram illustrating the mechanism of action of this antimicrobial cyclopeptide is presented in **Error! Reference source not found.**.

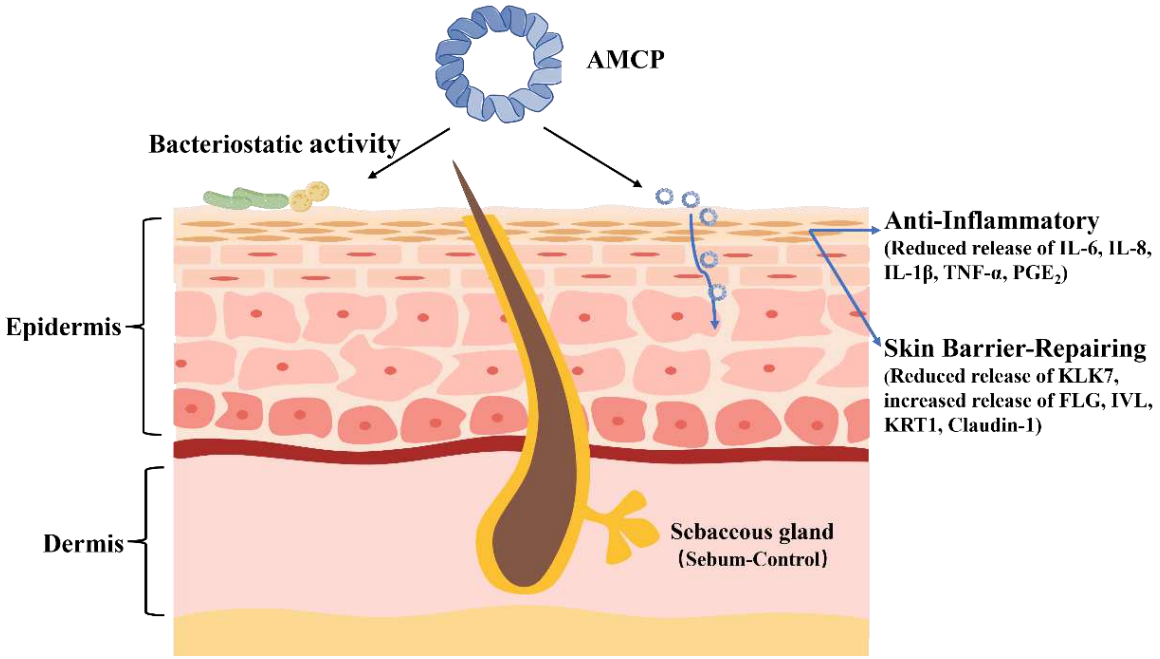

Figure 11. Schematic Illustration of the Anti-acne Mechanism of the AMCP. AMCP exerts its anti-acne effects through four key mechanisms: inhibiting sebum secretion, reducing the activity of *C. acnes* and *S. aureus*, suppressing the release of inflammatory factors, and promoting skin barrier repair. In addition, the use of penetration enhancers facilitates the transdermal delivery of AMCP, thereby significantly improving its therapeutic efficacy.

The androgen-mediated increase in sebum production is regarded as an essential step in the early pathophysiology of acne vulgaris.[23] DHT is a potent androgen that stimulates sebum secretion by binding to androgen receptors (ARs) located within sebaceous gland cells.[24] Therefore, a model of lipid overaccumulation was established in SZ95 cells by stimulation with DHT. The results showed that treatment with 15 μg/mL DHT significantly promoted lipid accumulation in SZ95 cells. In contrast, AMCP reduced lipid levels in a concentration-dependent manner. Notably, at a concentration of 20 μg/mL, AMCP achieved an inhibition rate of 40%. Fatty acids such as oleic acid, linoleic acid, and palmitic acid are typical lipid-derived stimulants that upregulate peroxisome proliferator-activated

receptors (PPARs), thereby stimulating sebocyte differentiation and promoting lipid synthesis in sebocytes.[25] Based on this, an in vitro model of lipid accumulation was also established in LA-stimulated SZ95 sebocytes to evaluate the inhibitory effect of AMCP on lipid synthesis. While treatment with 100 μg/mL LA significantly promoted lipid accumulation, AMCP reduced lipid levels in a concentration-dependent manner, achieving an inhibition rate of 29.1% at 20 μg/mL. These findings demonstrate that AMCP effectively suppresses DHT- and LA-induced lipid production in SZ95 cells, supporting its potential therapeutic application in the treatment of acne.

Acne is associated with dysbiosis of C. acnes and S. aureus.[26] Among which, *C. acnes* serves as the key pathogenic bacterium in acne vulgaris.[27] When C. acnes overproliferates within the hair follicle, it secretes lipases that hydrolyze triglycerides into pro-inflammatory free fatty acids, which subsequently trigger comedogenesis and promote inflammatory responses.[28,29] *S. aureus* is a commensal Gram-positive pathogenic bacterium coccus commonly found on the skin and mucous membranes. Although it does not serve as an initiating factor in acne, it can lead to secondary infection following impairment of the skin barrier caused by acne lesions. In this study, the in vitro antibacterial activity of AMCP was evaluated by determining the MIC and MBC against *C. acnes* and *S. aureus* using the broth microdilution method. The results showed that AMCP exhibited significant in vitro antibacterial activity against both strains. AMCP demonstrated strong bactericidal activity against *C. acnes*, with MIC and MBC values both determined to be 0.5 μg/mL. Notably, this activity surpassed that of minocycline, which exhibited an MIC of 3.125 μg/mL against the same strain.[30] The MIC and MBC of AMCP against *S. aureus* were both 1.0 μg/mL, demonstrating potent bactericidal activity that far surpassed that of clindamycin (MIC = 64 μg/mL) against the same strain.[31] Consequently, AMCP demonstrated considerable promise as an effective agent for ameliorating acne vulgaris.

Far from being a simple secondary outcome of follicular obstruction, acne is a chronic inflammatory skin disease, with inflammation serving as a pervasive factor throughout its entire course.[32] During

the early stages, under the influence of microenvironmental stimuli, hyperproliferation of keratinocytes and aberrant immune activation lead to the release of inflammatory mediators such as IL-6, thereby directly inducing follicular hyperkeratinization and initiating the formation of microcomedones.[33,34] The proliferation of *C.acnes* further amplifies inflammatory responses, driving the robust release of pro-inflammatory factors such as TNF-α and IL-8.[35] These key pro-inflammatory factors not only exacerbate local tissue damage by recruiting leukocytes but also act synergistically on the sebaceous glands to further stimulate sebum hypersecretion and induce the release of PGE_2.[36]To establish an in vitro inflammation model, HaCaT and SZ95 cells were stimulated with 1×10^7 CFU/mL of heat-killed *C. acnes*, respectively. Exposure to heat-killed *C. acnes* resulted in a significant elevation of IL-6, IL-8, PGE_2, IL-1β, and TNF-α secretion in both cell types. AMCP treatment markedly suppressed the levels of these inflammatory mediators. In HaCaT keratinocytes, the observed reductions were 81.0%, 90.1%, 64.6%, 93.1%, and 96.4%, while in SZ95 sebocytes, the decreases reached 84.8%, 89.1%, 33.4%, 91.2%, and 92.1%. These results suggested that AMCP exerted its anti-inflammatory action by suppressing the secretion of pro-inflammatory cytokines triggered by *C. acnes*, highlighting its potential to mitigate inflammation at its onset.

The occurrence of acne is closely linked to impaired skin barrier function.[37] Impairment of the skin barrier can induce or exacerbate acne, while the inflammatory response associated with acne, in turn, further compromises barrier integrity. Skin barrier repair is a dynamic process involving the coordinated action of multiple key proteins: IVL, a scaffold protein, acts as a molecular bridge between lipids and corneocytes;[38] FLG serves as a source of natural moisturizing factors (NMFs) upon degradation and plays a crucial role in maintaining skin water content;[39] Claudin-1 regulates tight junctions to achieve rapid barrier closure;[40] KRT1 provides cytoskeletal support;[41] and KLK7 regulates normal desquamation of the stratum corneum, with its activity requiring precise control to prevent excessive degradation.[42] Therefore, the expression levels of IVL, FLG, Claudin-1, KRT1, and KLK7 mRNA in HaCaT cells with and without AMCP treatment were compared using RT-PCR

in this study. The results revealed that AMCP treatment led to a concentration-dependent upregulation of IVL, FLG, Claudin-1, and KRT1 mRNA expression, but a downregulation of KLK7 mRNA expression in HaCaT cells. Treatment with 15 μg/mL of AMCP resulted in increases of 104%, 37%, 30%, and 43% in IVL, FLG, Claudin-1, and KRT1 levels, respectively, with a 27% reduction in KLK7 expression. These findings demonstrated that AMCP can systematically and coordinately modulate the expression of genes of the skin barrier-related proteins through multi-target mechanisms, highlighting its potential in improving skin barrier function.

The low bioavailability of AMPs, including AMCPs, constitutes a critical bottleneck hindering their translation from potential molecules into effective products.[43] Surfactin, a Bacillus subtilis-derived biosurfactant comprising seven amino acids linked to a β-hydroxy fatty acid chain, is valued for its green, natural, mild, safe, and readily biodegradable properties. Surfactin has been demonstrated to induce changes in the secondary structure of membrane proteins and to increase membrane permeability [44,45], and it possesses excellent permeation-enhancing properties.[46] In this study, the sodium salt form of surfactin (sodium surfactin), which exhibited improved water solubility, was used for the experiments. The results demonstrated that a mixture of the permeation enhancer (2.0% propylene glycol + 0.1% sodium surfactin) exhibited the most effective penetration-promoting performance. At 8 h, the permeation efficiency of this group was five-fold than that of the control group. This finding provided a significant experimental basis and formulation development foundation for the efficient topical delivery of AMCP in anti-acne applications.

In summary, this study unveils an AMCP characterized by a tetra-dimensional synergistic mechanism encompassing sebum control, antibacterial activity, anti-inflammation, and barrier repair, thereby offering a new solution for active ingredient innovation in functional skincare. In synergy with its optimized delivery system, this ingredient establishes a solid scientific foundation for the development of highly effective and safe anti-acne cosmetics, demonstrating significant potential to drive innovation and advancement in the functional skincare industry.

Data Availability

Data from transcriptomics experiments have been deposited in NCBI's Gene Expression Omnibus and are available at the following URL:https://www.ncbi.nlm.nih.gov/bioproject/PRJNA1473534.

Author Contributions: N.Y. and G.W.: Conceptualization, methodology, formal analysis, writing—original draft. N.Y., L.Z., M.Z. and J.W.: Investigation, data curation. G.G., T.H., J.Y., and J.W.: Software, resources, supervision. G.W. and J.W.: Conceptualization, supervision, writing—review and editing. All authors take full responsibility for the entire content of this manuscript and approved its submission.

Funding Delaration：

This research work was accomplished with fund provided by DFSIN (Shanghai) Biotechnology Co., Ltd., China.

References

1. Ullah R.et al. Absence of GSTT1 and polymorphisms in GSTP1 and TP53 are associated with the incidence of acne vulgaris. *Skin Res Technol*.29, e13333, https://doi.org/10.1111/srt.13333 (2023).
2. Laclaverie, M. et al. Development and characterization of a 3D in vitro model mimicking acneic skin. *Exp Dermatol*, 30, 347-357,https://doi.org/10.1111/exd.14268 (2021).
3. Weber N. et al. Hop Extract Acts as an Antioxidant with Antimicrobial Effects against Propionibacterium Acnes and Staphylococcus Aureus. *Molecules*. 24(2), 223,https://doi.org/10.3390/molecules24020223 (2019).
4. Issa, N. et al. Recommendations to Improve Outcomes in Acne and Acne Sequelae: A Focus on Trifarotene and Other Retinoids. *Dermatol Ther (Heidelb)*.15, 563–577, https://doi.org/10.1007/s13555-025-01344-y (2025).
5. Farrah, G. & Tan, E. The use of oral antibiotics in treating acne vulgaris: A new approach. *Dermatol Ther*. 29, 377-384,https://doi.org/10.1111/dth.12370 (2016).
6. Barros, B., & Thiboutot, D. Hormonal therapies for acne. *Clin*. *Dermatol.* 35(2), 168-172,https://doi.org/10.1016/j.clindermatol.2016.10.009 (2017).
7. Barbieri, J. S., Spaccarelli, N., Margolis, D. J., & James, W. D. Approaches to limit systemic antibiotic use in acne: Systemic alternatives, emerging topical therapies, dietary modification, and laser and light-based treatments. *J. Am. Acad. Dermatol*. 80(2),538-549,https://doi.org/10.1016/j.jaad.2018.09.055 (2019).
8. Reynolds, R. V.et al. Guidelines of care for the management of acne vulgaris. *J. Am. Acad. Dermatol*. 90, 1006.e1-1006.e30 (2024).
9. Pomi, F. L., Vaccaro, M., Peterle, L., & Borgia, F. Photodynamic therapy for severe acne. *Photodiagnosis Photodyn. Ther*. *45*, 103893,https://doi.org/10.1016/j.pdpdt.2023.103893 (2024).
10. Schoenberg, E., Wang, J. V., Zachary, C. B., & Saedi, N. Treatment of acne scars with PRP and laser therapy: an up-to-date appraisal. *Arch Dermatol Res*. 311, 643–646,https://doi.org/10.1007/s00403-019-01936-7 (2019).
11. Hassan, M.et al. Antimicrobial Proteins: Structure, Molecular Action, and Therapeutic Potential. *Pharmaceutics.* 15(1), 72, https://doi.org/10.3390/pharmaceutics15010072 (2023).
12. Hassan, M., Flanagan, T. W., Kharouf, N., Bertsch, C., Mancino, D., & Haikel, Y. Nanosystems as Vehicles for the Delivery of Antimicrobial Peptides (AMPs). *Pharmaceutics* .11(9), 448,https://doi.org/10.3390/pharmaceutics11090448 (2019).
13. Ribeiro, R., Pinto, E., Fernandes, C., & Sousa, E. Marine Cyclic Peptides: Antimicrobial Activity and Synthetic Strategies. *Mar. Drugs*. 20(6), 397,https://doi.org/10.3390/md20060397 (2022).
14. Lee, D. W., & Kim, B. S. Antimicrobial cyclic peptides for plant disease control. *Plant Pathol. J*. 31(1),1-11,https://doi.org/10.5423/PPJ.RW.08.2014.0074 (2015).
15. Fazili, T., Bansal, E., Garner, D., Gomez, M., & Stornelli, N. Dalbavancin as sequential therapy for infective endocarditis due to Gram-positive organisms: a review. *Int. J. Antimicrob. Agents*. 61(4), 106749,https://doi.org/10.1016/j.ijantimicag.2023.106749 (2023).
16. Tang, X.et al. Reassessment of the Broth Microdilution Method for Susceptibility Testing of Helicobacter pylori, *Clin. Dermatol*. 226(Supplement_5), S486-S492, https://doi.org/10.1093/infdis/jiac389 (2022).
17. Lee, J. D., Kim, J. Y., Jang, H. J., Lee, B. M., & Kim, K. B. Percutaneous permeability of 1-phenoxy-2-propanol, a preservative in cosmetics, *Regul. Toxicol. Pharmacol*. 103, 56-62,https://doi.org/10.1016/j.yrtph.2019.01.002 (2019).
18. Miner, K., et al. Lipid Dysregulation in Sebaceous Gland Disorders and the Impact of Sphingolipid Metabolism on Acne Pathogenesis. *Cureus*. 17(4), e82463, (2025).
19. Cong, T. X., Hao, D., Wen, X., Li, X. H., He, G., & Jiang, X. From pathogenesis of acne vulgaris to anti-acne agents. *Arch Dermatol Res*. 311, 337–349, https://doi.org/10.1007/s00403-019-01908-x (2019).

20. Beringer, A., Noack, M., & Miossec, P. IL-17 in Chronic Inflammation: From Discovery to Targeting, *Trends Mol. Med.* 22(3), 230-241,https://doi.org/10.1016/j.molmed.2016.01.001 (2016).
21. Chen, C.W.et al. Anti-inflammatory activity of α-tomatine via inhibition of the MAPK and NF-κB signaling pathway in vitro and ex vivo. *Int. J. Med. Sci.* 3(1), 194-203,https://www.medsci.org/v23p0194.htm (2026).
22. Deng, Y., Wang, F., & He, L. Skin barrier dysfunction in acne vulgaris: pathogenesis and therapeutic approaches. *Med. Sci. Monit.* 30, e945336, (2024).
23. Bungau, A. F., Radu, A. F., Bungau, S. G., Vesa, C. M., Tit, D. M., & Endres, L. M. Oxidative stress and metabolic syndrome in acne vulgaris: Pathogenetic connections and potential role of dietary supplements and phytochemicals. *Biomed. Pharmacother.* 2023,164,115003, https://doi.org/10.1016/j.biopha.2023.115003 (2023).
24. Kircik, L. H. Androgens and acne: perspectives on clascoterone, the first topical androgen receptor antagonist. *Expert Opin. Pharmacother.* 22(13), 1801–1806, https://doi.org/10.1080/14656566.2021.1918100 (2021).
25. Bharti, S., & Vadlamudi, H. C. A strategic review on the involvement of receptors, transcription factors and hormones in acne pathogenesis. *J. Recept. Signal Transduct.* 41(2), 105–116,https://doi.org/10.1080/10799893.2020.1805626 (2021).
26. Abou-Rjeileh, U., Lock, A. L., & Contreras, G. A. Oleic acid promotes lipid accumulation in bovine adipocytes: the role of peroxisome proliferator-activated receptor alpha (PPARα) signaling. *Animal*. 19(5), 101505,https://doi.org/10.1016/j.animal.2025.101505 (2025).
27. Forraz, N.et al. The World's First Acne Dysbiosis-like Model of Human 3D Ex Vivo Sebaceous Gland Colonized with Cutibacterium acnes and Staphylococcus epidermidis. *Microorganisms*. 11(9), 2183,https://doi.org/10.3390/microorganisms11092183 (2023).
28. Bhatt, J., Kumar, V. J., & Chahat. Acne vulgaris: key insights, treatment, and future prospects. *Mol. Divers.* 30,143–178,https://doi.org/10.1007/s11030-025-11209-3 (2026).
29. Tax, G.et al. Propionic Acid Produced by Propionibacterium Acnes Strains Contributes to Their Pathogenicity. *Acta Derm Venereol*. 96 (1),43-49,https://doi.org/10.2340/00015555-2154 (2015).
30. Wan, K., Chen, D. & Ma, L. Microbial fermentation purification of Sapindus mukorossi extract solution and anti-acne effect of Lactobacillus Sapindus fermentation broth. *Fine chemicals.* 41(05),1076-1783, (2024).
31. NOVI, H., & YEVA, R. Sinergicity test of silver nanoparticles and clindamycin against Staphylococcus aureus. *Int. J. Res. Pharm. Sci.* 11(1),1192-1198, (2020).
32. Zouboulis, C. C., Jourdan, E., & Picardo, M. Acne is an inflammatory disease and alterations of sebum composition initiate acne lesions. *J. Eur. Acad. Dermatol. Venereol.* 28,527-532,https://doi.org/10.1111/jdv.12298 (2014).
33. Rübe, C. E., Freyter, B. M., Tewary, G., Roemer, K., Hecht, M., & Rübe, C. Radiation Dermatitis: Radiation-Induced Effects on the Structural and Immunological Barrier Function of the Epidermis. *Int. J. Mol. Sci.* 25(6),3320,https://doi.org/10.3390/ijms25063320 (2024).
34. Tu, Z.et al. IL-6 up-regulates expression of LIM-domain only protein 4 in psoriatic keratinocytes through activation of the MEK/ERK/NF-κB pathway. *Am. J. Pathol.*194, 708-720, (2024).
35. Lim, H. J., Kang, S. H., Song, Y. J., Jeon, Y. D., & Jin, J. S. Inhibitory Effect of Quercetin on Propionibacterium acnes-induced Skin Inflammation. *Int. Immunopharmacol*. 96,107557,https://doi.org/10.1016/j.intimp.2021.107557 (2021).
36. Tang, Y.et al. Prostaglandin E2 alleviates inflammatory response and lung injury through EP4/cAMP/IKK/NF-κB pathway. *Biochim Biophys Acta Mol Basis Dis.* 1871(5),167801,https://doi.org/10.1016/j.bbadis.2025.167801 (2025).
37. Dull, K. et al. Barrier function-related genes and proteins have an altered expression in acne-involved skin. *J.*

Eur. Acad. Dermatol. Venereol. 37,1415–1425,https://doi.org/10.1111/jdv.19062 (2023).

38. Yang, R.et al. Protective Effect of Peony (Paeonia ostii) Flower Extract Against Tape Stripping-Induced Skin Barrier Impairment in Mice. *Molecules*. 31(1),62, https://doi.org/10.3390/molecules31010062 (2026).
39. Sumitomo, A.et al. Phenylalanine amide derivatives promote FLG expression via AHR activation in normal human epidermal keratinocytes. *J. Pharmacol. Sci.* 159(1), 44-53,https://doi.org/10.1016/j.jphs.2025.06.005 (2025).
40. Bergmann, S. et al. Claudin-1 decrease impacts epidermal barrier function in atopic dermatitis lesions dose-dependently. *Sci Rep*. 10, 2024,https://doi.org/10.1038/s41598-020-58718-9 (2020).
41. Winkler R.et al. The Adhesion G-Protein-Coupled Receptor GPR115/ADGRF4 Regulates Epidermal Differentiation and Associates with Cytoskeletal KRT1. *Cells*. 11(19):3151,https://doi.org/10.3390/cells11193151 (2022).
42. de Veer, Simon J.et al. Selective substrates and inhibitors for kallikrein-related peptidase 7 (KLK7) shed light on KLK proteolytic activity in the stratum corneum. *J. Invest. Dermatol.* 137, 430-439, (2017).
43. Sakai, T. Stratum Corneum Ceramide Abnormalities in Atopic Dermatitis: Pathophysiology and Implications for Disease Management. *J. Dermatol.* 53,380-387, https://doi.org/10.1111/1346-8138.70098 (2025).
44. Zhang, L., Xing, X., Ding, J., Zhao, X., & Qi, G. Surfactin variants for intra-intestinal delivery of insulin. *Eur. J. Pharm. Biopharm.* 115, 218-228,https://doi.org/10.1016/j.ejpb.2017.03.005 (2017).
45. Zhang, L., Gao, Z., Zhao, X., & Qi, G. A natural lipopeptide of surfactin for oral delivery of insulin. *Drug Deliv*. 23(6), 2084–2093,https://doi.org/10.3109/10717544.2016.1153745 (2016).
46. Lee, B. M., Jang, B. J., Shin, J. A., & Shin, H. S. Enhancement of transdermal permeation of phycobiliprotein by nanodispersion with lipopeptide from Bacillus subtilis. *Biotechnol. Bioprocess Eng.* 30(2),401-410,https://doi.org/10.1007/s12257-024-00166-7 (2025).